Effects of the fourth component and undercooling on morphology of primary Mg-Zn-Y icosahedral quasicrystal phase under normal casting conditions

***Wang Zhifeng[1], Zhao Weimin[1], Bo-Young Hur[2], Huang Chunying[1]and Yu Chengquan[1]**

(1. School of Materials Science and Engineering, Hebei University of Technology, Tianjin 300130, China; 2. School of Nano and Advanced Materials Engineering, Gyeongsang National University, Jinju 660-701, Korea)

Abstract: The paper presents some results of the investigation on effects of the fourth component (Ti, C, Sb or Cu) and undercooling on the morphology, size and forming process of primary Mg-Zn-Y icosahedral quasicrystal phase (I-phase) under normal casting conditions. The result shows that the addition of certain amount of fourth component can transform I-phase morphology from petal-like to spherical. However, I-phase will grow up to petal-like if superfluous addition of the fourth component applied. It is also found that the solidified morphology of I-phase depends on the stability of spherical I-phase during the subsequent growth, and critical radius of maintaining the spherical I-phase interface relatively stable. Further, mini-sized spherical I-phase can be produced with high content of the fourth component by undercooling. Such findings are beneficial for industrializing Mg-based quasicrystals.

Key words: magnesium alloy; quasicrystal; fourth component; morphology; degree of undercooling
CLC number: TG146.2+2 Document code: A Article ID: 1672-6421(2009)04-293-07

Since the discovery of the first icosahedral quasicrystalline (IQC) structure in a rapidly solidified Al-Mn alloy by Shechtman et al. [1], icosahedral quasicrystalline phases (I-phases) were reported in many alloy systems [2,3]. I-phases offer attractive properties, such as high strength, high corrosion resistance, high thermal conductivity, low interfacial energy and low friction coefficient due to its special crystal structure [4,5], but their innate brittleness and intricate preparation method inhibited their application as structural materials. A new approach having been developed to expand the application of quasicrystals, is to prepare metal matrix composites reinforced with the quasicrystalline phases [6-8]. In 1993, Luo[9] et al. discovered stable icosahedral quasicrystalline phases in as-cast Zn-Mg-RE alloys, which indicates that quasicrystalline phase can be easily obtained under normal casting conditions, and this new alloy system contains a wide range for forming quasicrystalline phases. Moreover, the new quasicrystals can be produced under normal casting conditions instead of rapid solidification process. Nowadays, an industrial-scale production of quasicrystals-containing materials is taking place throughout the world.

Since the beginning of the new millennium, different components of the Mg-Zn-RE alloy system have been designed by researchers [10-14]. For example, Zhang [15, 16] et al., through study on the effect of Mn and Ca on the morphology and macrohardness of Mg-Zn-Y alloys, found out that with the increase of Mn or Ca, IQC became more spherical with decreased microhardness. Such research contributes to developing new quarternary Mg-based IQC. The purpose of the present work was to systematically study the effects of the fourth component (Ti, C, Sb or Cu) and undercooling on morphology, size and forming process of Mg-Zn-Y primary IQC under normal casting conditions.

1 Experimental

Alloys of nominal composition listed in Table 1 were melted using a crucible electric resistance furnace (SG2-5-10A) under the mixture of SF_6/CO_2 protective atmosphere using 99.95% Mg, 99.90% Zn, 99.95% Y, 99.99% Cu, 99.99% C nanotubes, Mg-20%Ti master alloy and Mg-25%Sb master alloy (wt.%). The schematic diagram of apparatus for making quasicrystal alloys in this work is shown in Fig.1. Stirring for 5 min at 800℃ and holding for 30 min at 780℃, the melt was then poured into a cast iron mould preheated to 300℃, as shown in Fig.2(a), and cooled with mould in water. The microstructures of the specimens were investigated with scanning electron microscope (SEM, Philips XL30, Netherlands) equipped with energy-dispersive spectroscopy

***Wang Zhifeng**

Male, born in 1982, doctoral candidate. His research interests mainly focus on light alloys and their forming technology. He was the excellent member of CCP of Hebei University of Technology in 2007-2008, bestowed upon Top Graduate Student Award of Hebei University of Technology in 2008 and Hebei Provincial Scientific and Technological Achievement Award (First place) in 2009. He has written 4 technical papers.
E-mail: zhifeng_wang@yahoo.com
Received: 2008-11-25; Accepted: 2009-06-28

(EDS). The phases were identified by X-ray diffraction (XRD, Rigaku 2500/PC, Japan) using monochromatic Cu-K-radiation. Icosahedral quasicrystalline structure was identified by means of transmission electron microscopy (TEM, Philips F20, Netherlands) operating at 120 kV.

Table 1 Nominal compositions and comparisons of the experimental alloys

Alloy No.	Alloy compositions					Size of I-phase (μm)	Morphology of primary I-phase
	Mg	Zn	Y	Fourth component	Content (at. %)		
1	72.0	26.5	1.5	–	–	10–12	Petal-like
2	72.0	26.0	1.5	Ti	0.5	7–10	Spherical
3	72.1	26.2	1.5	C	0.2	4–7	Spherical
4	72.2	26.2	1.5	Sb	0.1	5–8	Spherical
5	72.1	26.2	1.5	Sb	0.2	10–17	Petal-like
6	72.1	26.2	1.5	Cu	0.2	23–28	Petal-like
7	72.0	26.0	1.5	Cu	0.5	1.5–3.0	Spherical

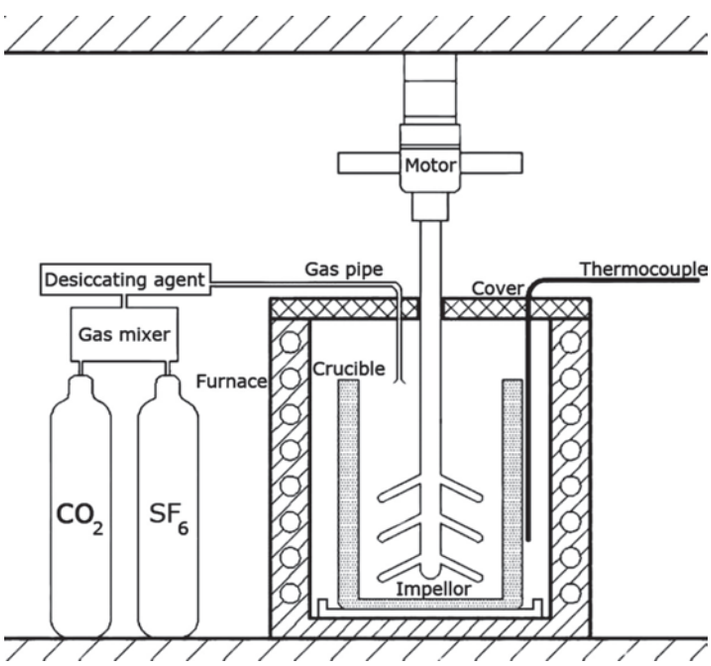

Fig. 1: Schematic diagram of apparatus for making quasicrystal alloys

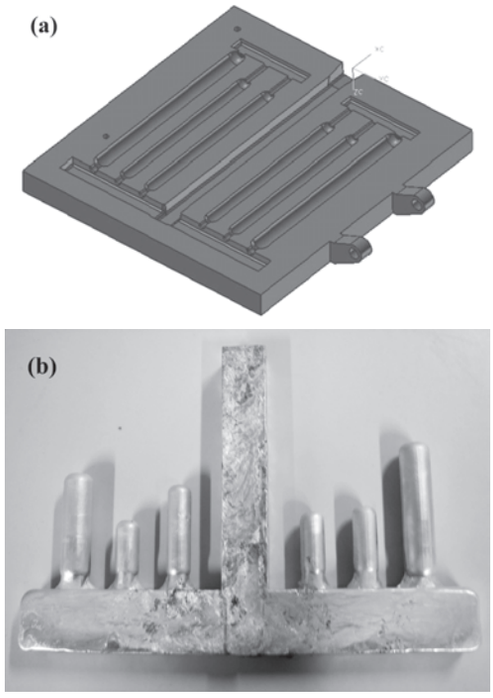

Fig. 2: Sketch map of cast iron mould (a) and its casting (b)

2 Results and discussion

2.1 Microstructures of experimental alloys

A typical micrograph of Alloy No.1 is shown in Fig.3(a). The solidification microstructure of the alloy consists of four different phases: petal-like phases, lamellar eutectic structures, black particles and gray matrix phase (marked by arrows). Only three phases, i.e., *a*-Mg, I-phase and Mg_7Zn_3 phase, were identified with XRD, as shown in Fig.3(b). EDS result indicates that the black particles surrounding the primary phase and the eutectic structure are *a*-Mg solid solution, the gray matrix phase is Mg_7Zn_3, and petal-like phases are I-phase. Electron diffraction pattern confirmed that the petal-like phase is indeed the I-phase with typical selected area electron diffraction (SAED) patterns at fivefold, threefold and twofold axes (Fig.3e–g). Very different from the 32 kinds of classical crystal point groups, the point group of IQC exhibits (or 532)[17]. Thus, with this special point group, as for quasicrystal, it is possible to distinguish this dense diffraction pattern from classical crystals. Besides, petal-like I-phase was clearly found to be surrounded by lamellar eutectic phases, as shown in the TEM micrograph (Fig.3d). EDS analysis shows that the average composition of I-phase is Mg-58.3Zn-6.1Y, and that of eutectic structure is Mg-25.8Zn-3.6Y. Obviously, Y content of eutectic structure is lower than that of I-phase, and the Mg content of eutectic structure is higher than that in I-phase. As a matter of fact, the eutectic structure consisting of *a*-Mg and I-phase has been reported previously [4,11]. Although I-phase existed in both petal-like phases and lamellar eutectic phases, petal-like phases were primary I-phases. The research focus in this study was on morphology, size and microhardness of these primary I-phases and their formation process.

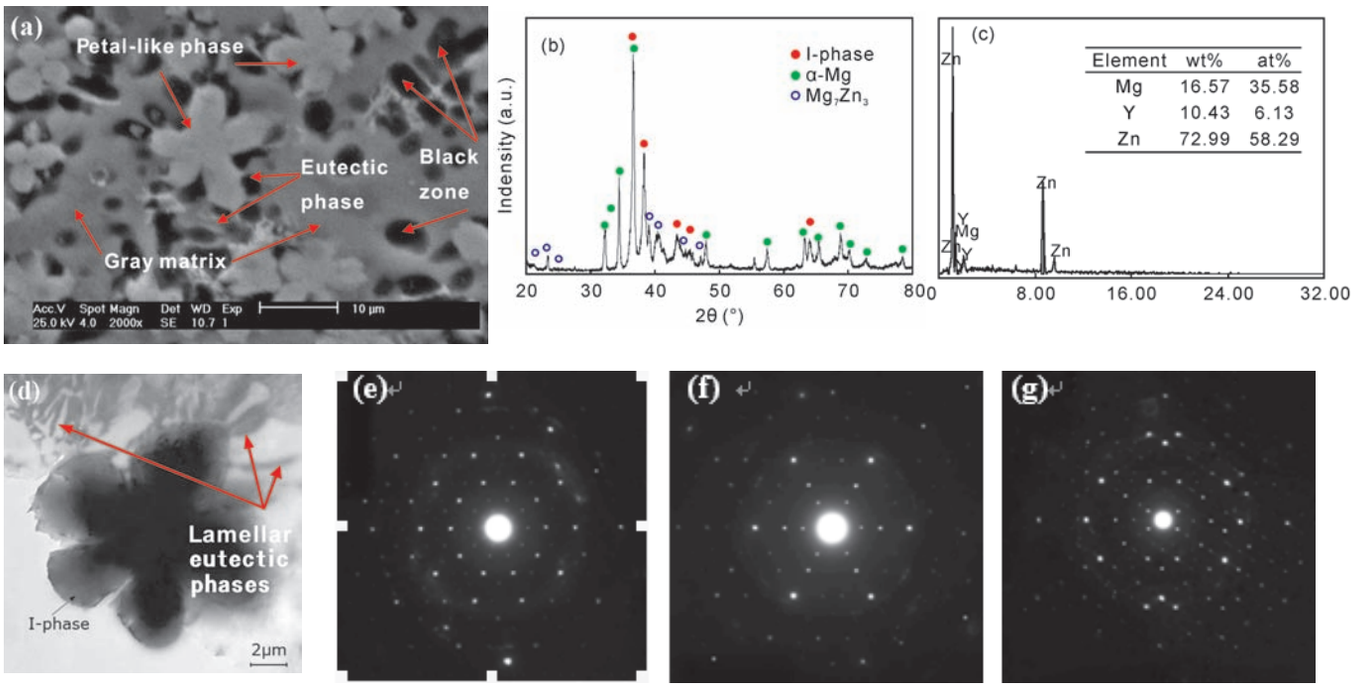

Fig.3: SEM image (a), XRD patterns (b), EDS analysis of I-phase center (c), TEM image (d), SAED patterns (e)–(g) with fivefold, threefold and twofold, respectively, for as-cast Alloy No.1 containing IQC

Ti and C were introduced respectively into Mg-Zn-Y alloy under the same casting condition as Alloy No.1. SEM micrographs of I-phase in Alloy No.2 and Alloy No.3 are shown in Figs.4 (a) and 4(b), respectively. XRD analysis of Figs. 4(c) and 4(d) show that I-phase substantially exists in both alloys. EDS analysis of Figs. 4(e) and 4(f) shows that spherical I-phase consists of four components, i.e. Mg, Y, Ti, Zn in Alloy No. 2, Mg, Y, C, Zn in Alloy No. 3. Moreover, the SAED patterns at fivefold axes of spherical I-phases in Alloy No.2 and Alloy No.3, as shown in Figs.4(g) and 4(h), respectively, confirmed icosahedral quasicrystal phases of the quaternary spherical Mg-Zn-Y-X(X=Ti, C). Thus, the significant function of the fourth component is to transform the morphology of I-phase from petal-like to spherical. Similar phenomenon were observed when Cu, Sb, Mn[15] or Ca[16] were added into Mg-Zn-Y alloy.

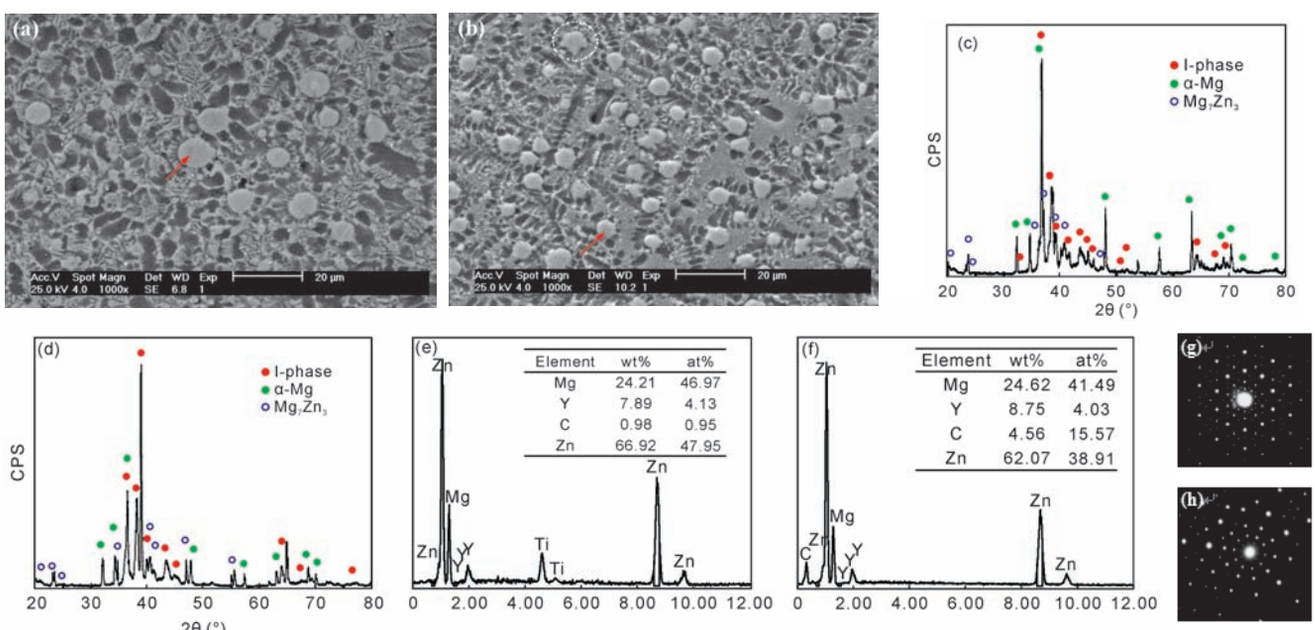

Fig.4: SEM images of Alloy No.2 (a) and No.3 (b) containing spherical IQC; XRD analysis of Alloy No.2 (c) and Alloy No.3 (d); EDS analysis of spherical IQC marked by arrows in (a) and (b), (e): Alloy No.2, (f): Alloy No.3; fivefold axes SAED patterns of I-phase, (g): Alloy No.2, (h): Alloy No.3

2.2 Formation mechanism of spherical IQC

The solidification processes are different for forming quasicrystals and amorphous phase. Moreover, the solidification process of quasicrystal phases which consists of grain nucleation and their subsequent growth is similar to that of crystals forming process [20]. So, it is necessary to properly control the cooling rate for the formation of the quasicrystal

phase, which was thermodynamically unstable. Lower cooling rate might not effectively suppress the crystallization and would result in the formation of crystal phase while higher cooing rate might suppress the nucleation and growth of the quasicrystal phase and would result in the formation of amorphous phase. However, for quasicrystal-containing magnesium alloys, stable I-phase can be obtained under normal casting conditions. Therefore, the main critical factors affecting the formation of Mg-based I-phase were alloying composition, diffusion and coalescence of alloy elements and their crystalline structure types except from the cooling rate [21].

Some researches consider that cooling rate had no significant effect on the nucleation process of Mg-based I-phase[15,21], while the subsequent growth of I-phase at local undercooling region in the melt had close relation with the distribution of alloy elements at the solidification front. Due to the coalescence of the fourth component at solidification front, surface energy at that local region was elevated and growing velocity of I-phase slowed down. Moreover, the same heat dissipating condition in all directions lead to the same growing velocity of I-phase in all directions, thus making the final morphology of I-phase of Alloy No.2 and No.3 spherical.

At the early stage of nucleation process, the single fourth component particles act as potential nucleating substrates, and the morphology of I-phase should be nearly spherical as the result mentioned above. During this process, the highest volume percentage of surface layer to the whole volume of I-phase particle resulted in the highest surface energy of I-phase, which enabled the morphology of I-phase particle shrinking to spherical or near-spherical. Therefore, the solidification morphology of I-phase depended on the stability of spherical I-phase during the subsequent growth. I-phase with spherical morphology would be obtained if I-phase forming initially could preserve spherical interface stable in the whole growth process. Otherwise, I-phase with irregular or dendrite morphology would be eventually generated. According to Mullins et al. [22, 23], relative stability criterion of spherical interface with radius being Rr can be expressed by the rate of change per unit perturbation amplitude:

$$\frac{\dot{\delta}}{\delta} \leqslant \frac{\dot{R}}{R} \tag{1}$$

$$\frac{\dot{\delta}}{\delta} = \frac{(l-1)K_l}{K_s L}\left[\Delta T - \Gamma\frac{T_m\Gamma}{R}(1+\partial_t)\right] \tag{2}$$

The critical radius maintaining the spherical I-phase interface relative stable was:

$$R_r = \frac{2T_m\Gamma}{\Delta T}\left[1+\frac{(l-1)}{(l-2)}\partial_t\right] \tag{3}$$

$$\partial_t = \frac{1}{2}(l+2)\left[1+l\left(1+\frac{K_s}{K_l}\right)\right] \tag{4}$$

Where, δ, K_s, K_l, L, ΔT, Γ, l and T_m are the amplitude of fluctuation, the thermal conductivity of the solid phase, the thermal conductivity of the liquid phase, latent heat of freezing, degree of undercooling in the melt, the ratio of interface energy to latent heat of solid phase per unit volume, the rank of spherical harmonic function, the melting point of the alloy, respectively.

It can be seen from Eqs. (3) and (4) that decreasing ΔT or elevating the interface energy between the I-phase and the melt are beneficial to the stability of spherical interface. The addition of the fourth component not only provided potential nucleating sites for I-phase, but also purified the melt by removing oxygen and forming compound of Ti with harmful impurity elements. The coalescence of the fourth component compounds at solid/liquid interface resulted in higher interface energy and higher value of Γ. Moreover, the addition of the fourth component promoted heterogeneous nucleation of I-phase, lowered the local melt front undercooling ΔT and increased the critical radius R_r. Meanwhile, the same heat dissipating condition of the I-phase particle in all directions resulted in the same growing velocity of I-phase particle in all directions, enabling I-phase to keep spherical growing front and providing positive conditions for spherical growth of I-phase.

$$\Delta T = \Delta T_h + \Delta T_c + \Delta T_k \tag{5}$$

Where, ΔT_h, ΔT_c, ΔT_k, are thermodynamics undercooling, the constitutional undercooling, and the kinetics undercooling, respectively. It means that ΔT is composed of three parts of ΔT_h, ΔT_c and ΔT_k.

The fourth component C is active impurity element. The addition of a small amount of active carbon brought about kinetics undercooling, improved ΔT and finally decreased R_r. If the exact radius of IQC is bigger than R_r, I-phase with irregular or petal-like morphology would be eventually generated, as shown in Fig.5(b) marked by arrows. For most IQC particles, the exact radius of IQC was smaller than R_r although R_r decreased a little, and spherical morphology would be finally created owing to spherical interface kept stable in the subsequent growth process.

2.3 Functions of different contents of the fourth component and different degree of undercooling

As discussed above, the addition of the fourth component resulted in transformation of morphology of I-phase from petal-like to spherical. However, if superfluous addition of the fourth component, un-dissolved fourth component will be discharged from the solid phase to solid/liquid interface and formed the fourth component solute transitional layer with certain thickness. Moreover, due to the increasingly enrichment of the fourth component compounds in front of the growing solid/liquid interface of I-phase particle, the degree of constitutional undercooling increased, and ΔT increased as well. Increased ΔT intensified the instability of spherical growing surface of I-phase particle. Then the I-phase will turn to coarsen, the spherical morphology will be wrecked and transform to petal-like.

Figures 5(a) and (b) show the Mg-Zn-Y-0.1(at. %)Sb

and Mg-Zn-Y-0.2(at. %)Sb alloys. The SAED patterns of I-phase in Fig.5 are fivefold axes. So, we can confirm that the phases marked by red arrows in Fig.5 are indeed the I-phases. Furthermore, the I-phase morphology of Alloy No. 4 was spherical while Alloy No. 5 presented petal-like one again. It can be seen from Fig.5(a) that the value of critical radius R_r of I-phase of Alloy No. 4 was about 8 μm when the content of the fourth component Sb was 0.1%. If local conditions changes, and spherical radius value exceeds R_r, the transformation of morphology of I-phase from spherical to petal-like will occur (marked by the lower red arrow in Fig.5(a). So we can see that the superfluous addition of the fourth component has negative effect on the stability of spherical interface, and also is adverse to forming spherical I-phase. One can also see from Fig.5(b) that most of I-phases are petal-like while a few of I-phase are spherical (marked by white arrows). Therefore a critical stable radius indeed exists. Once the interface radius of I-phase is greater than R_r in IQC growth process, the final morphology of I-phase in that local zone will be petal-like. On the other hand, spherical morphology will be preserved in local zone if the interface radius of I-phase is smaller than R_r.

The effect of different contents of the fourth component

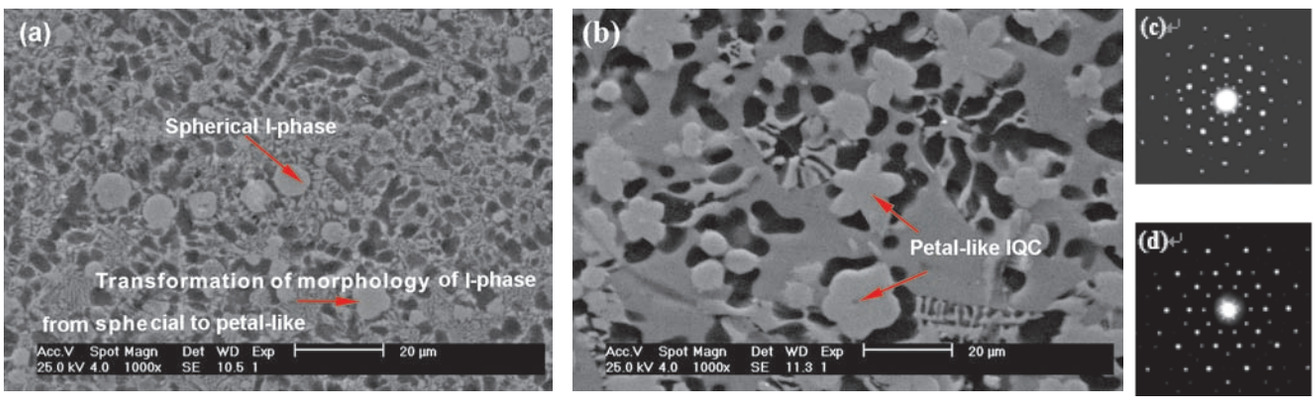

Fig.5 SEM image of as-cast Alloy No.4 (a) and No.5 (b) containing I-phase and fivefold axes SAED patterns of I-phase in Alloy No.4 (c) and Alloy No.5 (d).

and different degree of undercooling on critical stable radius of spherical I-phase is schematically shown in Fig.6. As discussed previously, under certain cooling condition with proper compositions of Mg-Zn-Y alloys, certain size of critical stable radius exists and we describe this state as state I. The addition of a small amount of the fourth component results in an decrease of undercooling and finally increases the critical stable radius R_r as seen in Eqs.(3). We can describe this state

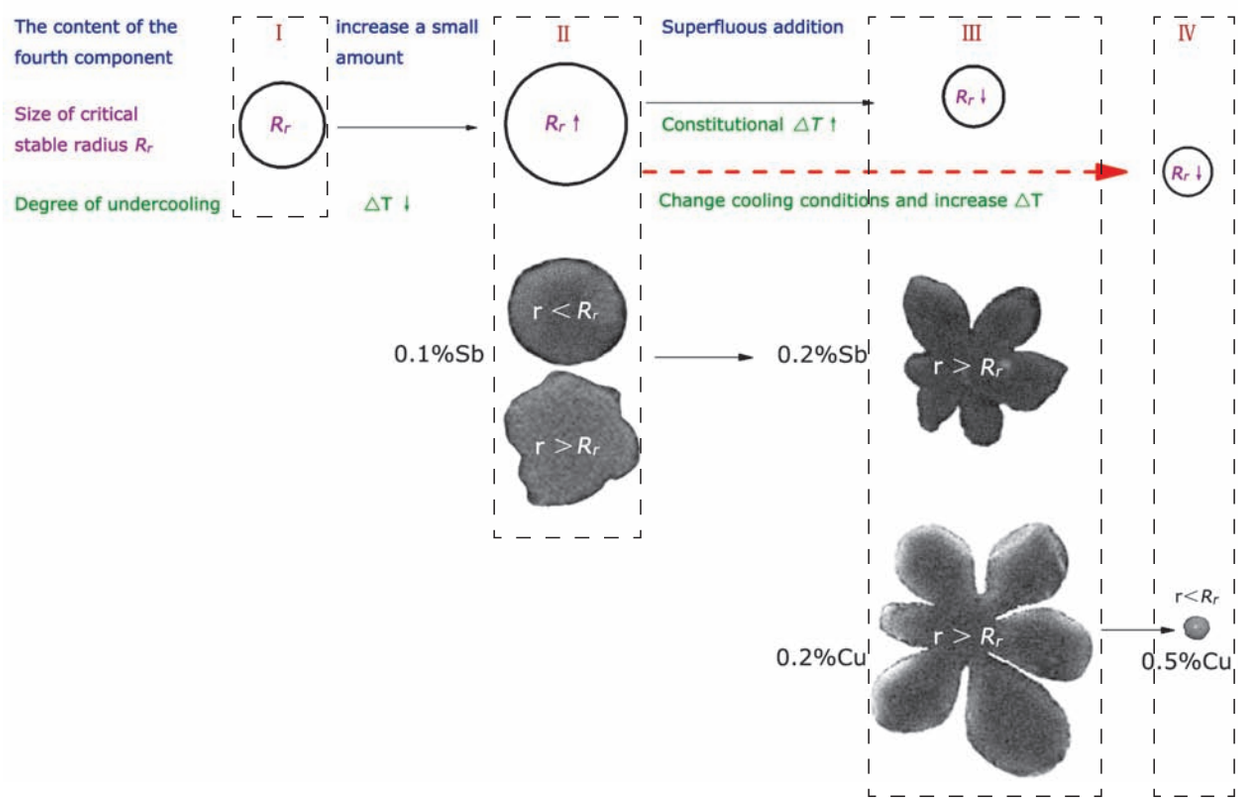

Fig.6: Schematic diagram of different states and change process of critical stable radius

as state II. However, if superfluous addition of the fourth component, constitutional undercooling becomes significant, ΔT will increase. Thus the critical stable radius of spherical I-phase will decrease. This state is called state III.

It is proposed that the type of fourth component and its corresponding critical stable radius depend on cooling condition and type of alloys. Figure 6 shows the example of fourth component as Sb or Cu. Spherical IQC can only be formed when the radius of IQC is less than R_r in their respective states. Under most of conditions, if superfluous addition of the fourth component, small-sized R_r will generate big-sized petal-like IQC. It seems as if superfluous addition of the fourth component could not produce spherical I-phase. Actually, we can improve cooling conditions and increase ΔT_h and also ΔT by thermodynamics method. Much smaller critical stable radius will make it difficult to forming spherical I-phase. However, higher cooing rate might cut down the growth time of the quasicrystal phase. Spherical interface of I-phase forming at preliminary stage will be stably preserved in the whole growth process, and then smaller-sized spherical I-phase with radius less than *R*r will occur. We can define this state as state IV. Under such a theoretical framework, with high content of the fourth component, spherical I-phase with amazingly small size, as shown in Fig.7(b), can be produced by using a water cooling copper mould equipment, as shown in Fig.8(a). XRD analysis in Fig.7(c) shows that I-phase substantially exists. EDS analysis of Figs.4(e) and 4(f) show that spherical I-phase consists of four components. Moreover, the SAED patterns at fivefold axes of spherical I-phases in Alloy No.7 were shown in Fig.7(f). Thus, the quaternary spherical Mg-Zn-Y-Cu icosahedral quasicrystal phases were confirmed. So, it is a novel way to form spherical I-phase with high content of the fourth component with refined size by increasing thermodynamics undercooling ΔT_c. In this way, we can easily control cooling rate in a certain range and obtain quarternary spherical IQC at different length scale.

3 Conclusions

(1) The addition of fourth component resulted in transformation of morphology of I-phase from petal-like to spherical. The solidified morphology of I-phase depends on the stability of spherical I-phase during the subsequent growth and critical radius of the spherical I-phase interface relative stable.

(2) Superfluous addition of the fourth component has negative effect on the stability of spherical interface and leads to bigger interface radius than critical stable radius. Whereafter, the I-phase will grow up to petal-like. Spherical IQC is only formed when the radius of IQC is less than *R*r in their respective states.

(3) Refined quarternary spherical I-phase can be produced by improving thermodynamics undercooling and with high content of the fourth component.

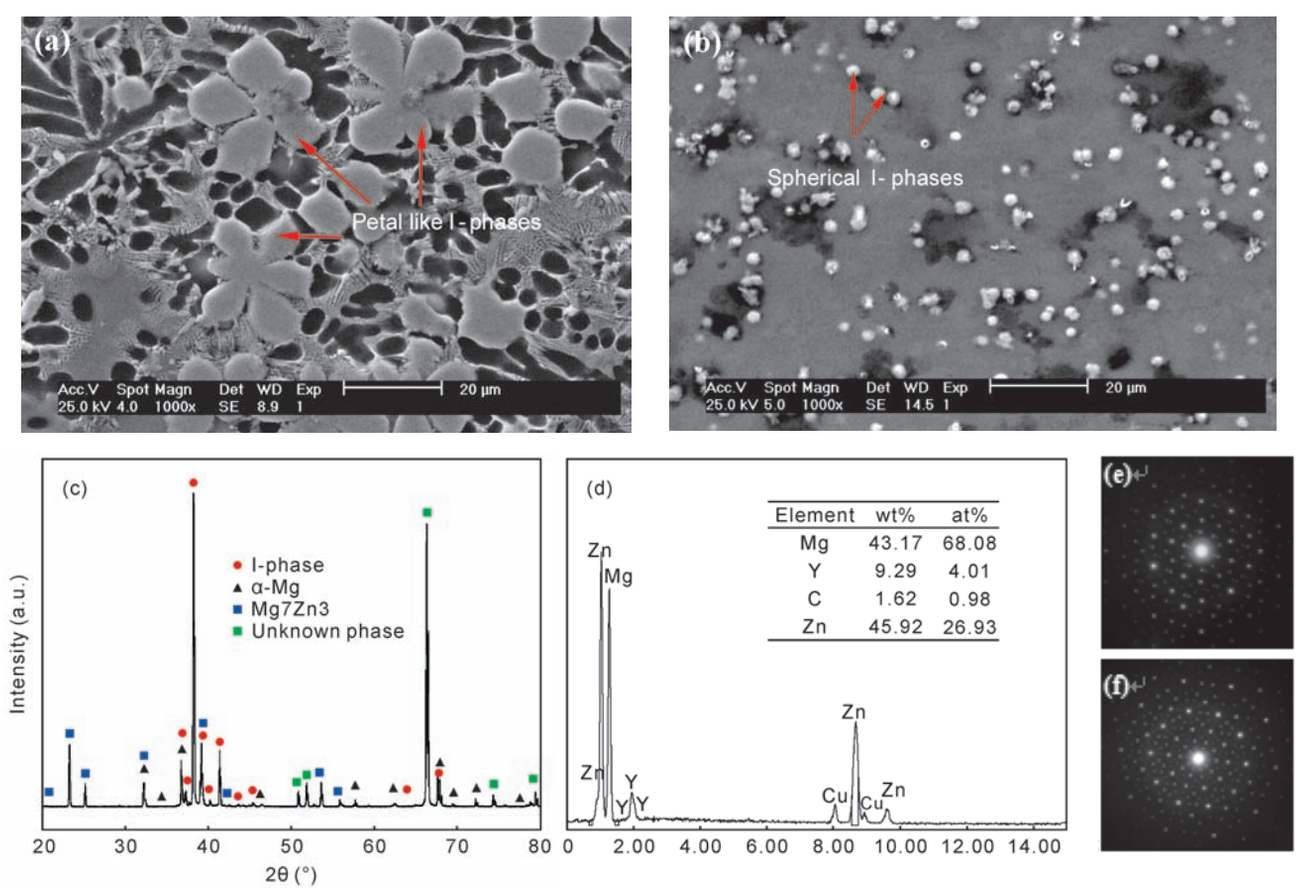

Fig.7: SEM images of Alloy No.6 (a) and No.7 (b) containing I-phases , XRD analysis of Alloy No.7 (c), EDS analysis of spherical I-phase in Alloy No.7 (d), and fivefold axes SAED patterns of I-phase in Alloy No.6 (e) and Alloy No.7 (f)

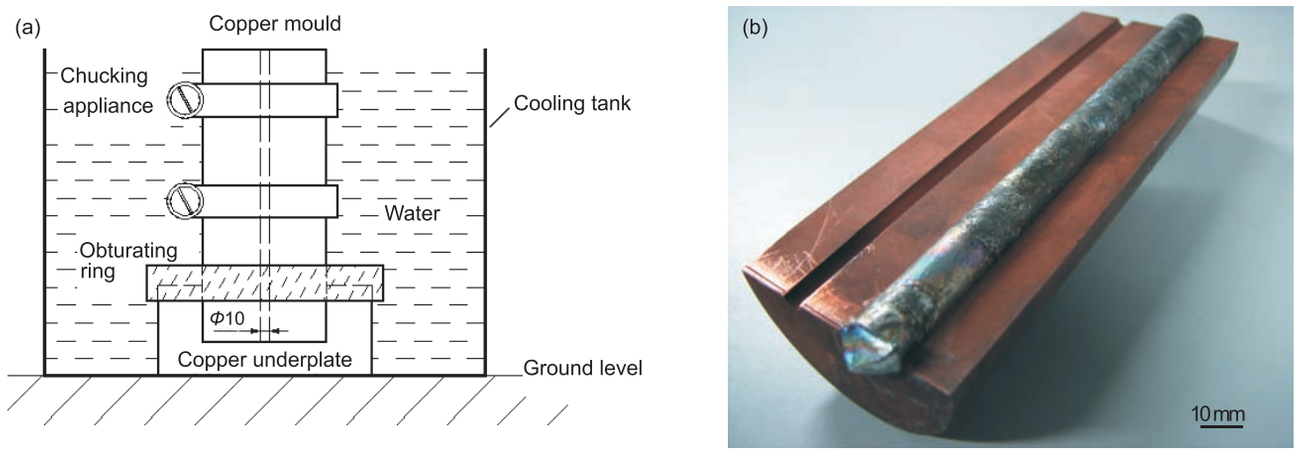

Fig. 8: Sketch map of copper mould (a) and its casting (b)

References

[1] Shechtman D, Blech I, Gratias D, Chan J W. Metallic phase with long-range orientational order and no translational symmetry. *Physical Review Letters,* 1984, 53(20): 1951–1953.

[2] Tsai An-Pang, Inoue Akihisa, Masumoto Tsuyoshi. A Stable Quasicrystal in Al-Cu-Fe System. *Jpn. J. Appl. Phys.,* 1987, 26: L1505–L1507.

[3] Sastry G V S, Rao V V, Ramachandrarao P, Anantharaman T R. A new quasi-crystalline phase in rapidly solidified Mg_4CuAl_6. *Scripta Metallurgica*, 1986, 20:191–193.

[4] Zhang Yingbo, Yu Sirong, Zhu Xianyong, Luo Yanru. Study on as-cast microstructures and solidification process of Mg-Zn-Y Alloys. *J. Non-Cryst. Solids,* 2008, 354: 1564-1568.

[5] Köster U, Liu W, Liebertz H, Michel M. Mechanical properties of quasicrystalline and crystalline phases in Al-Cu-Fe alloys. *J. Non-Cryst. Solids,* 1993, 153: 446–452.

[6] Singh Alok, Watanabe M, Kato A, Tsai A P. Strengthening in magnesium alloys by icosahedral phase. *Science and Technology of Advanced Materials,* 2005, 6: 895–901.

[7] Zhang Yingbo, Yu Sirong, Song Yulai, Zhu Xianyong. Microstructures and mechanical properties of quasicrystal reinforced Mg matrix composites. *Journal of Alloys and Compounds,* 2008, 464(1-2): 575–579.

[8] Bae D H, Lee M H, Kim K T, Kim W T, Kim D H. Application of quasicrystalline particles as a strengthening phase in Mg-Zn-Y alloys. *Journal of Alloys and Compounds*, 2002, 342: 445–450.

[9] Luo Zhiping, Zhang Shaoqing, Tang Yali, et al. Ouasicrystals in as-cast Mg-Zn-RE alloys. *Scripta Metallurgica et Materialia,* 1993, 28(12): 1513–1518.

[10] Wan Diqing, Yang Gencang, Zhu Man, et al. Solidification of Mg-28%Zn-2%Y alloy involving icosahedral quasicrystal phase. *Trans. Nonferrous Met. Soc. China*, 2007, 17: 586–589.

[11] Yi S, Park E S, Ok J B, et al. (Icosahedral phase + α-Mg) two phase microstructures in the Mg-Zn-Y ternary system. *Materials Science and Engineering A*, 2001, 300: 312–315.

[12] Lee Ju Yeon, Kim Do Hyung, Lim Hyun Kyu, et al. Effects of Zn/Y ratio on microstructure and mechanical properties of Mg-Zn-Y alloys. *Materials Letters*, 2005, 59: 3801–3805.

[13] Xiao Wenlong, Wang Jun, Yang Jie, et al. Microstructure and mechanical properties of Mg-12.3Zn-5.8Y-1.4Al alloy. *Material Science and Engineering A,* 2008, 485: 55–60

[14] Bae D H, Kim Y, Kim I J. Thermally stable quasicrystalline phase in a superplastic Mg-Zn-Y-Zr alloy. *Materials Letters*, 2006, 60: 2190–2193.

[15] Zhang Jinshan, Du Hongwei, Liang Wei, et al. Effect of Mn on the formation of Mg-based spherical icosahedral quasicrystal phase. *Journal of Alloys and Compounds*, 2007, 427: 244–250.

[16] Zhang Jinshan, Du Hongwei, Lu Binfeng, et al. Effect of Ca on crystallization of Mg-based master alloy containing spherical quasicrystal. *Trans. Nonferrous Met. Soc. China*, 2007, 17, 273–279.

[17] Luo Zhiping, Zhang Shaoqing, Tang Yali, Zhao Dongshan. On the stable quasicrystals in slowly cooled Mg-Zn-Y alloys. *Scripta Metallurgica et Materialia*, 1995, 32(4): 1411–1416.

[18] Wan Diqing, Yang Gencang, Chen Sulin, et al. Growth morphology and evolution of quasicrystal in as-solidified Y-rich Mg-Zn-Y ternary alloys. *Rare Metals,* 2007, 26(5): 435–439.

[19] Wan Diqing, Yang Gencang, Lin lin, Feng Zhigang. Equilibrium and non-equilibrium microstructures of Mg-Zn-Y quasicrystal alloy. *Materials Letters*, 2008, 62: 1711–1714.

[20] Chen Guang, Fu Hengzhi, Sun Guoyuan, et al. *Novel Metal Materials with Non-equilibrium Solidification*. Beijing: Science Press, 2004, 112–113. (in Chinese)

[21] Shi Fei, Guo Xuefeng, Zhang Zhongming. Quasicrystal of as-cast Mg-Zn-Y alloy. *The Chinese Journal of Nonferrous Metals,* 2004, 14(1): 112–116.

[22] Mullins W W, Swkerka R F. Morphological stability of a particle growing by diffusion or heat flow. *Journal of Applied Physics*. 1963, 34(2): 323.

[23] Min Naiben. *Physical Fundamental of Crystal Growth*. Shanghai: Shanghai Scientific and Technical Press, 1982, 163–165. (in Chinese)

This work was supported by the Natural Science Fund of Hebei Province (E2008000045), and Doctoral Science Foundation of Hebei University of Technology.